Uranium Uptake by Montmorillonite-Biomass Complexes

Melisa S. Olivelli,[†,‡] Gustavo A. Curutchet,*[,‡,§] and Rosa M. Torres Sánchez[†,§]

[†]Centro de Tecnología de Recursos Minerales y Cerámica (CETMIC), Camino Centenario y 506, M.B. Gonnet, Buenos Aires, Argentina

[‡]Laboratorio de Análisis Ambiental, Escuela de Ciencia y Tecnología, Instituto de Investigación e Ingeniería Ambiental, Universidad Nacional de San Martín, Buenos Aires, Argentina

[§]CONICET, Consejo Nacional de Investigaciones Científicas y Tecnicas, Av. Rivadavia 1917 (C1033AAJ), Buenos Aires, Argentina

Ⓢ Supporting Information

ABSTRACT: Montmorillonite clays and biomass have noticeable metal sorption capacity. Clays or biomass are difficult to separate from the solution when used as sorbent materials. A methodology to retain biomass and improve separation processes is to generate clay biopolymers matrices from fungal biomass grown on a natural Montmorillonite (MMT). The objective of this study is to generate and characterize clay biopolymers matrices and evaluate their uranium adsorption capacity. The generated clay biopolymers (BMMTs) were characterized through X-ray diffraction, measurement of the apparent diameter of particles, and electrophoretic mobility. Some BMMTs showed greater Uranium-specific adsorption capacity than that found for MMT. The X-ray diffraction analysis indicated that the Uranium was located partially in the clay interlayer. The BMMT surfaces were more negatively charged than the MMT surface, thus favoring their uranium uptake. Also, immobilization of the biomass and better coagulation of the system were achieved. These preliminary studies indicate that BMMTs have a great potentiality for uranium uptake processes.

■ INTRODUCTION

Concern about the environment has led to the development of great number of investigations to remove pollutant agents, mainly from water and soil. Particularly, the extraction of uranium ore (to be used for the first part of the fuel cycle) generates large volumes of waste and effluents, coming from (i.e., in Argentina) the 5 000 000 tons of uranium extracted between 1952 and 2003.[1] However, these wastes are only slightly radioactive and need to be handled in the same manner as conventional treatments of metal-mining residues. Moreover, waste from mining activities presents metallic sulfides that can be oxidized leading to acidification of the surrounding waters and the release of metals.[2] Active mines pour liquid wastes, containing acids, metals, and residual uranium compounds to the neighboring streams. However, not only are active mines environmentally harmful but also inactive ones still have large leaching pads that release metallic wastes and this process is increased during the summer rainy season.[3]

Uranium typically occurs as hexavalent uranyl aqueous complexes in oxic environments.[4] U(VI) interacts with biotic and abiotic components of soils, which determine its mobility. In fact, extensive studies have been done on the interaction of U(VI) with fungi and bacteria[5,6] and with minerals.[7,8]

Generally, conventional remediation techniques for radionuclide removal from wastewaters are based in the use of coaly materials, ionic exchange resins, and chemical precipitation. However, due to the large volumes treated and the low concentration of pollutants, in addition to their costs, they are not suitable. Therefore, adsorption in low cost materials with high affinity for radionuclides, such as clays and biomass, represents an alternative of interest in wastewater treatments.[9,10]

Montmorillonite clays are minerals with great specific surface and optimal properties for metal adsorption.[11,12] They are also able to complex many kind of organic and polymeric compounds on its surface.[13,14] Particularly, the uptake of uranium from aqueous solutions by the use of montmorillonites was demonstrated.[15,16]

However, some problems arise with the use of these clays in processes of metal adsorption from aqueous solution. The small particle size ($<2~\mu m$) and colloidal characteristic of montmorillonite made difficult their separation from the aqueous phase.[17] Also, it was indicated that the sedimentation capability of organo modified montmorillonites was improved respect to that of raw montmorillonites.[18] Then, the separation of these clay systems from the solution after a remediation process could be achieved.

Biosorption is an alternative process where different types of biomass allow to concentrate radionuclides from diluted solutions.[9] Mixtures of bacterial biomass and kaolinite clay were used to study the uranium adsorption[19] and references therein. The fungal biomass was among one of the most commonly used biosorbents, with the advantage of being easily and low cost generated.[9] Again, the main technological drawback is the separation process. To solve this issue, immobilization of the biomass on an adequate innocuous material was proposed.[20]

Knowledge of the mechanisms of metals and other contaminants uptake by biomass associated to matrixes found in natural environments such as clays and sediments is very important to understanding the processes involved in its fate in natural environments and to develop remediation alternatives for polluted water. For this reason, the use of uranium resistant strains for biofilm formation in adverse conditions is necessary.
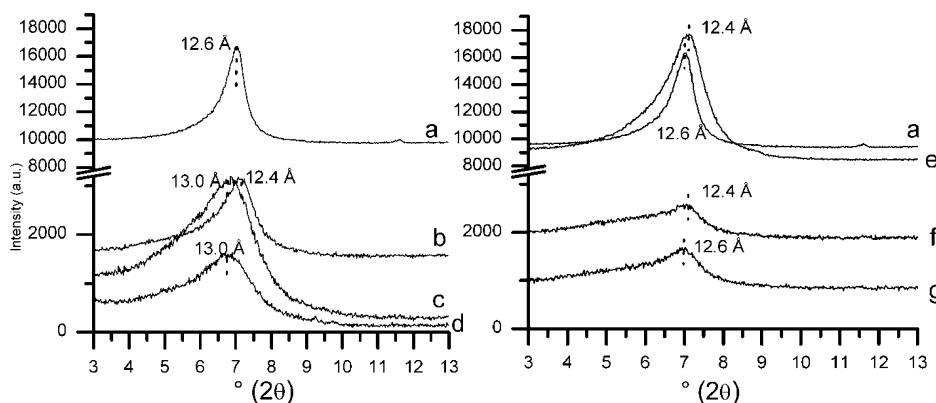
The aim of the present study is to evaluate the generation of montmorillonite biopolymers (BMMTs) as a novel methodology to increase the biosorption capacity and retain biomass and

Figure 1. Partial XRD patterns of indicated samples: (a) MMT; (b) MMT 1% (P5); (c), BMMT 1% (*Acre* sp.); (d) BMMT 1% (*Apha* sp.); (e) MMT 5% (P5); (f) BMMT 5% (*Acre* sp.); (g) BMMT 5% (*Apha* sp.).

uranium uptake, improving the coagulation properties of the system that leads to an easier separation of the solids from the solution. The BMMT samples and those with uranium absorbed were characterized by apparent particle diameter, X-ray diffraction (XRD), and ζ-potential determinations.

EXPERIMENTAL SECTION

Materials. A bentonite sample (MMT) coming from the Argentine North Patagonia (Rio Negro) was used as raw material. The MMT mineralogy was evaluated by X-ray diffraction and chemical analysis in previous works[13,21] and consists of Na-rich montmorillonite (>99%) with minor phases as quartz and feldspars. Some physicochemical parameters of the raw MMT were determined elsewhere: structural formula $[(Si_{3.89} Al_{0.11})(Al_{1.43}Fe^{3+}_{0.28}Mg_{0.30})O_{10}(OH)_2] M^+_{0.41}$;[22] cationic exchange capacity (CEC) = 174 meq/100 g clay, isoelectric point (IEP) at pH = 2.7, and specific surface area determined by N_2 adsorption (Brunauer−Emmett−Teller (BET) method) $S_{N2} = 34.0 m^2 g^{-1}$ and $S_w = 621 m^2 g^{-1}$.[23]

Two uranium resistant fungi genus were used: *Aphanocladium* sp. (*Apha* sp.) and *Acremonium* sp. (*Acre* sp.). To generate clay biopolymers (named as BMMT (*Apha* sp.) or BMMT (*Acre* sp.)), the biomass were grown axenically during 5 days, in batch systems with P5 culture medium (1.28 g/L K_2HPO_4; 3 g/L $(NH_4)_2SO_4$; 0.25 g/L $MgSO_4\cdot7H_2O$; 10 g/L glucose; 0.1 g/L thiamine; 1% (v/v) cations solution; 1% (v/v) anions solution) containing MMT clay 1% (w/v) or 5% (w/v) and the same amount of initial inoculums (pH 5.5, 25 °C). Generated BMMTs were recovered by centrifugation (20 min, 2200 g, 4 °C) and washed with distilled water. Images from scanning electronic microscopy of BMMT (*Apha* sp.) samples are given as an example of BMMTs morphology in the Supporting Information (Figures S1 and S2).

Characterization Methods. The water molecules' adsorption was determined, at relative humidity (rh) 0.56, as described elsewhere.[24] Biomass sites for water adsorption are not specifically determined as in clays, so this parameter does not indicate the specific surface in the biopolymers generated (as in montmorillonites).

Different matrices samples without and with uranium adsorbed (U-BMMTs) were analyzed by X-ray diffraction (XRD) on oriented samples, to obtain an accurate peak analysis, prepared by spreading the sample suspension on glass slides and dried at room temperature overnight with atmospheric humidity control, rh = 0.47. Analyses were performed using a Philips PW 1710 diffractometer using Cu Kα radiation. The work conditions

were power supply at 40 kV and 30 mA, 1° divergence and detector slits, 0.02° (2θ) step size, counting time of 10 s/step, and patterns collected from 3° to 14° (2θ). The d(001) peaks from U-BMMTs XRD spectra were decomposed using the origin Pro 7.0 software (fitting wizard method) taking into account Gaussian functions.[25] The fit quality was controlled by the R^2 value (>0.98).

The electrophoretic mobility and the apparent diameter were determined with a Brookhaven90Plus/Bi-MAS equipment, in the mode ζ-potential and Multi Angle Particle Sizing, respectively, operating at $\lambda = 635$ nm, 15 mW solid state laser, scattering angle 90°, temperature 25 °C, and using KCl 10^{-3} M as inert electrolyte.

The content of organic matter was determined by thermal treatment at 600 °C for 3 h of the BMMT samples.

Total proton consumption was determined on suspensions of 0.13% (w/v) of each sample. All suspensions had an initial pH of around 4.5. The amount of HNO_3 0.02 M consumed to reach pH 2.8 was determined. The experiments were duplicated, and the error was taken as 5% of the values.

Adsorption Experiments. Uranyl nitrate solutions containing 10, 25, 50, 100, 150, 200, and 250 ppm uranium pH 3.6 were prepared (0.04, 0.1, 0.21, 0.42, 0.63, 0.84, 1.05 mM uranium, respectively). The experiments were carried out three times as independent experiments, and each isotherm concentration had four replicates. Biopolymer samples (0.1 g) were shaken for 2.25 h (according to previous equilibrium essays, data not shown) in polypropylene tubes with 10 mL aliquots of each solution. After the equilibration time, two samples of 1 mL were taken from each tube and centrifuged (5000 g, 8 min). The supernatant was analyzed for uranium with the Arsenaze (III) technique,[26] and the solid was reserved for XRD and electrophoretic mobility analysis. The metal adsorbed was calculated as the difference between the initial concentration and that of the supernatant in equilibrium. The uranium adsorption capacity was fitted by Langmuir, Freundlich, and sigmoidal isotherms, using the Sigma-Plot 10.0 software (Statistics—Regression Wizard).

RESULTS AND DISCUSSION

Characteristics of Montmorillonite/Biomass Complexes. Analysis of XRD spectra of montmorillonite sample indicated the presence of a water monolayer in the interlayer space which originates a reflection peak (001) at 12.6 Å,[27,28] while the presence of the sterile P5 culture medium generated a displacement of this peak toward 12.4 Å, indicating a light interlayer space compression (Figure 1). This behavior could be

originated by the ionic strength (around 0.2 M) of the P5 culture medium used to grow the fungal biomass, which remove water molecules from the montmorillonite interlayer generating its shrinkage.[29]

In the BMMTs with 1% the (001) reflection peak shift toward 13.0 Å indicating an interlayer expansion respect to that of MMT, while in BMMTs with 5% of MMT, the interlayer showed a compression (12.4 Å), similar to that found in the MMT (P5) systems (Figure 1). The biomass growth could prevent the interlayer shrinkage caused by the effect of the ionic strength from the culture medium, where the interaction with the interlayer cations provoked this expansion. The mechanisms involved need further research.

The water molecules different interaction forces with MMT, BMMTs, and biomass do not allow calculating the specific surface from the values of water molecules adsorption.[24] The water mass adsorbed for *Acre* sp. and *Apha* sp. (117 ± 5 and 82 ± 3 mg H_2O/g respectively) were in the same order of magnitude of the values obtained for MMT and MMT (P5) (87 ± 1 and 65 ± 2 mg H_2O/g, respectively). This could be indicating that their surface functional groups interact with water molecules similarly. The differences of water mass values for MMT and MMT (P5) samples indicated that less water molecules are adsorbed in the MMT (P5) sample in agreement with the interlayer shrinkage found by XRD. The adsorbed water by BMMT (*Acre* sp.) samples was lower than the values obtained for MMT or biomass alone (50 ± 2 and 72 ± 1 mg H_2O/g for 1 and 5%, respectively). BMMT (*Apha* sp.) samples (52 ± 1 and 72 ± 1 mg H_2O/g for 1 and 5%, respectively) showed the same behavior. These observations suggested that properties of generated biopolymers are not a sum of the properties of MMT and biomass. Values between samples of BMMTs with both species did not show significant differences, probably due to the similar growth type that presented both fungi genus in the presence of MMT as Supporting Information.

Table 1 shows the values for organic matter of BMMTs samples as biomass content, data from proton consumption as

Table 1. Biomass Content and Total Proton Consumption

sample	biomass content (mg biomass/g BMMT)	mmol H^+/ g sample	(mmol H^+ BMMT − mmol H^+MMT)/g biomass in BMMT
MMT		0.6	
Acre sp.		1.2	1.2
Apha sp.		1.2	1.2
MMT 1% (P5)		0.21	
MMT 5% (P5)		0.22	
BMMT 1% (*Acre* sp.)	237	1.2	2.5
BMMT 5% (*Acre* sp.)	57	0.9	5.2
BMMT 1% (*Apha* sp.)	257	1.3	2.7
BMMT 5% (*Apha* sp.)	73	0.95	4.7

mmol HNO_3 per gram of sample, and proton consumption as mmol HNO_3 per gram of biomass.

BMMT samples with higher content of MMT (BMMTs with 5% of MMT) evidenced lower biomass/clay relation (Table 1), notwithstanding that all samples contain the same total amount of biomass to generate clay biopolymers (all flasks were inoculated with the same amount of inoculums and have the same amount of carbon and energy source). This fact has effects in

proton consumption behavior. The quantity of consumed protons (mmol H^+/g matrix) was higher in biomass than in MMT (Table 1). Despite the value of water adsorption capacity of MMT was higher than those for BMMTs, the total proton consumption of the studied materials indicated that there were more available sites to exchange protons in BMMTs than in MMT in the studied pH range (pH of interest in uranium adsorption, from 4.5 to 2.8). Also, the quantity of exchangeable sites on MMT (P5) was lower than on MMT. In BMMT samples, this property increased according to the biomass/clay relationship (Table 1). Indeed, an analysis of the proton consumption of BMMTs per unit of biomass (proton consumption attributed to biomass in the BMMT structure, for calculation see Supporting Information) increased when the proportion of biomass in the BMMT sample was lower. This fact, together with the scanning electronic microscopy, suggests a different configuration of the biomass in the structure of each BMMT. A network of biomass can be seen in both BMMT, but in the sample of 1% (Figure S1, Supporting Information), it is noticed how the biomass is grouped by sectors, while in the 5% (Figure S2, Supporting Information) samples it is much more evenly distributed.

This increase of the proton consumption capacity of BMMTs, with respect to that of MMT and biomass alone, demonstrates that clay biopolymers have an advantageous structure for chemisorption processes.

There are no differences (within the error method) found between Dapp values of MMT and BMMT samples. Biomass could be growing in the MMT surface, but the size of the particle remains constant indicating no-aggregation. *Acremonium* sp. and *Aphanocladium* sp. biomass growing alone forms stable and high size aggregates that were difficult to separate from the solution by decantation or centrifugation (Table S1 and Figure S4, Supporting Information).

ζ-Potential Curves. To determine the existence of electrostatic surface changes in MMT (mainly in the edges surfaces[30]) by the culture medium, or biomass growth, it was measured the ζ-potential values in a pH range from 3 to 8 for MMT, MMT (P5), *Apha* sp., and BMMT (*Apha* sp.). Data is represented in Figure 2A.

The similarity of MMT and MMT (P5) ζ-potential curves indicated that edges surface charge was not highly affected by the increase of ionic strength. *Apha* sp. ζ-potential data indicated that, in the pH range 3.5 to 6, the fungi surface was negatively charged, increasing the surface negative charge with the pH. This behavior is in agreement with that found for other fungi genus[31] and assigned to a complex mixture of chemical moieties. These may include carboxyl groups as the most significant group involved.[32]

Particularly, at pH 3.5, the ζ-potential value of BMMTs was around −40 mV, while for MMT and *Apha* sp. they were −30 and −10 mV, respectively. The increase in the negative surface charge of BMMTs with respect to MMT, up to pH 6.5, could be explained by an electrostatic attraction of the fungi genus (negative charge) to the edges of the MMT (IEP of edges ≈ pH 6.5[33]). The reversal of the MMT edges charge sign at pH 6.5 does not maintain the previous electrostatic attraction, and the electric charge of the BMMTs equals the value obtained for MMT sample.

These behaviors were observed for both fungi (ζ-potential curves for *Acre* sp., not shown, were very similar to that of *Apha* sp.).

In addition to the electrostatic attractions determined by the ζ-potential data, hydrophobic forces have also been described related to biomass sorption on different surfaces.[34] Both
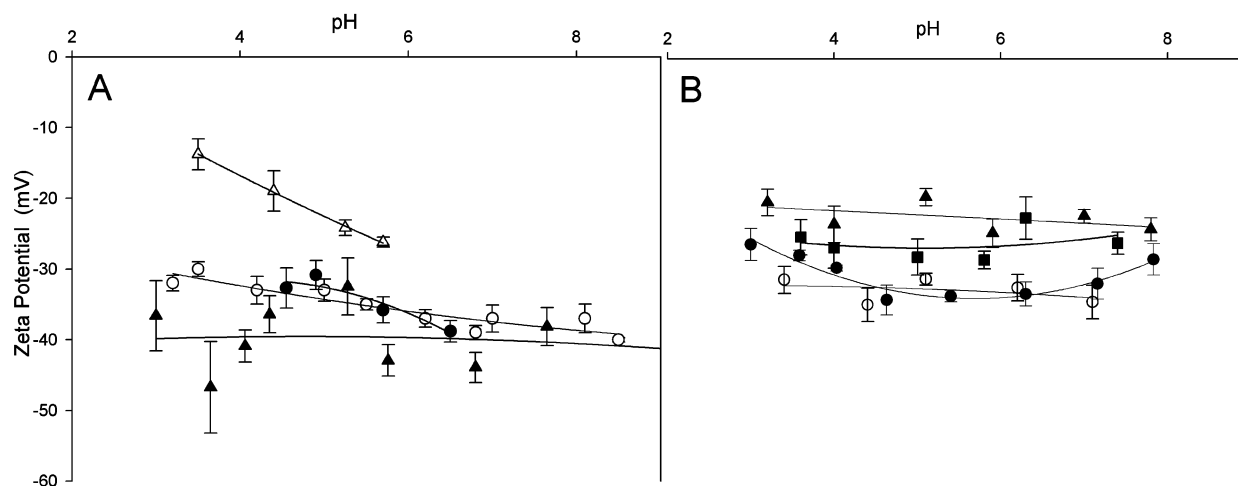
Figure 2. ζ-Potential curves: (A) without uranium; (B) with Uuranium. Symbols indicate: (○) MMT; (△) *Apha* sp.; (▲) BMMT 1% (*Apha* sp.); (●) MMT 1% (P5); (■) BMMT 1% (*Acre* sp.).
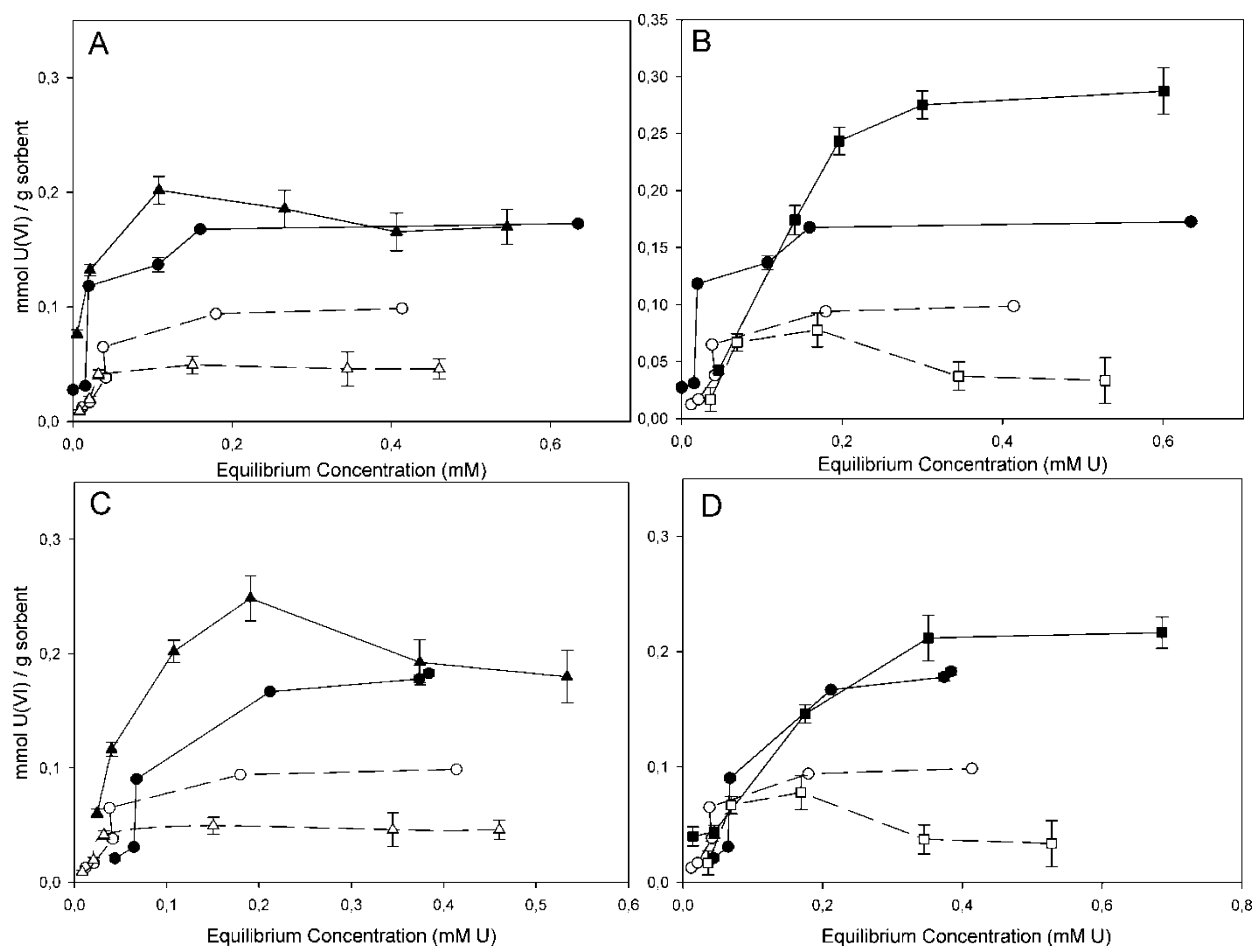
Figure 3. Uranium adsorbed on BMMT and respective controls: (A and B) BMMT in 1% w/v; (C and D) BMMT in 5% w/v. Symbols indicate: (○) MMT; (●) MMT (P5); (▲) BMMT (*Apha* sp.); (△) *Apha* sp.; (■) BMMT (*Acre* sp.); and (□) *Acre* sp.

electrostatic and hydrophobic forces may be partly responsible to the consequent improvement of the BMMT samples coagulation properties (Figure S4, Supporting Information).

Uranium Adsorption Isotherms. Figure 3 represents uranium adsorption isotherms using MMT, MMT (P5), and BMMT samples. For both BMMT samples, the adsorption

capacity of the system was higher than those of MMT or MMT (P5) samples. Also, a significant adsorption efficiency increase was found for BMMT samples compared with those of both biomasses alone (Figure 3).

Despite the results for the water adsorption values and proton consumption, the uranium adsorption in MMT (P5) was higher

2276

dx.doi.org/10.1021/ie301773p | *Ind. Eng. Chem. Res.* 2013, 52, 2273−2279

than the adsorption on MMT. The higher adsorption of uranium by MMT (P5) than MMT could be related with the preadsorbed organic matter (glucose and thiamine of the culture medium) that could not be removed after washing the samples in the sample preparation. Because of this effect, we compare all the isotherms together including those for MMT (P5). An experiment to quantify the influence of organic matter in MMT (P5) uranium adsorption was added. Isotherms with MMT (P5) and MMT (P5) without glucose and thiamine were performed (Supporting Information). The presence of organic matter such as glucose and thiamine could improve the uranium adsorption capacity of the system as MMT (P5) presented a higher U(VI) adsorption (Figure S5, Supporting Information).

The increase in the adsorption capacity of BMMT samples could be explained by an increase in the uranium adsorption affinity similarly to results found for the proton exchange capacity.

In previous experiences, it was shown that previously dried *Acre* sp. and *Apha* sp. biomass presented a higher uranium adsorption capacity than the adsorption capacity of wet systems.[35] This was explained in terms of a change in biomass conformation during the drying process, where more adsorption sites could be exposed. Our results were comparable with those found by Gargarello et al.[35] In both studies, wet biomass alone presented similar values (the differences could be due to the error method as the concentrations measured are too low). Also, wet BMMTs adsorption data showed slightly lower values reported for dried biomass[35] (being in the same order of magnitude) but with the advantage of being more easily separated from the solution. These similarities could be due to changes in the conformation of the biomass surface when growing with MMT as support material (Figure S1 and S2, Supporting Information), similarly as occurred in the drying process.

These results, along with the proton consumption data, suggest that biomass has a higher specific uranium adsorption capacity than MMT. This capacity was probably increased due to changes in the conformation, as mentioned. These changes could generate a mayor exposition of the functional groups responsible for chemisorption, increasing indeed the uranium and protons adsorption capacity.

Water adsorption results didn't show this effect suggesting the affinity of water molecules for other sites besides those for protons and uranyl binding.

Model Fitting. Several authors reported that heavy metals adsorption on MMT has a high correlation to the Langmuir isotherm.[36,37] Uranium adsorption on MMT also has a high correlation to the Langmuir equation, but our results could be explained as well by a different model such as a sigmoidal one. Experimental data indicated that BMMT samples did not fit to the Langmuir model (Table S2, Supporting Information) neither to Freundlich isotherms (data not shown). The sigmoidal shape of isotherms suggested different adsorption sites with different affinities for uranium or the existence of a cooperation effect, which increases the affinity between uranyl molecules and adsorption sites. The fit of experimental adsorption values to sigmoidal shape isotherms were resumed in Table S2 (Supporting Information).

A possible explanation for the high correlation to a sigmoidal model could be the heterogeneity of sites where the adsorbate can bind on the BMMT. Clays have interlayer spaces and external sites, and biomass surface functional groups could provide a larger quantity of metal binding sites and greater affinity to the system. Evidence of adsorption of uranium in interlayer space is shown below. Studies of U(VI) interactions with fungi and

bacteria showed that U(VI) may be associated with the functional groups on the cellular surface.[5,38,39]

XRD Spectra in the Presence of Uranium. Figure 4 shows the oriented XRD partial patterns of MMT sample without
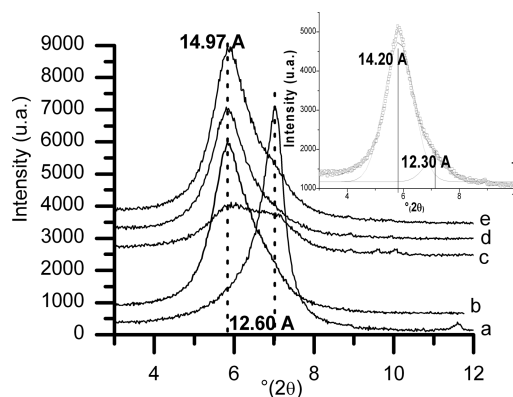
Figure 4. Partial XRD patterns of indicated samples: (a) MMT; (b) U-MMT; (c) U-BMMT 5% (*Apha* sp.); (d) U-BMMT 5% (*Acre* sp.); (e) U-MMT 5% (P5); and (f) U-BMMT 5% (*Acre* sp.).

uranium and samples in the presence of uranium. Last samples were recovered from an adsorption point of the isotherms (100 ppm, Figure 3).

A shift of the reflection peak d(001) toward smaller values of 2θ was observed for all the samples with uranium adsorbed respect to that found for samples without uranium (Figure 1). The shift of the reflection peak d(001), for all samples, to a constant value of 14.97 Å indicated the entrance of the uranyl cation to the clay interlayer.[7] Particularly, a study from Monte Carlo simulations indicated that uranyl ions formed outer-sphere surface complexes in the MMT interlayer with a tilt angle of around 45° to the surface normal.[15]

The asymmetrical shape of the reflection peak d(001) for all samples with uranium, compared to that of MMT sample and also to the respective samples without uranium (figure 1), indicated the existence of a heterogeneous interlayer. To achieve some precision of the latter behavior, the mathematical decomposition of the reflection peak d(001) for U-BMMT 5% (*Acre* sp.) sample was performed and shown as the inset of Figure 4 (Figure 4f). Similar peak behavior were found for U-BMMT 5 and 1% (Apha sp.) samples (data not shown), where the MMT increase, as in U-BMMT 5% (*Acre* sp.) sample, generated a right asymmetry in the reflection peak d(001).

Two symmetrical peaks were found for the d(001) reflection peak decomposition of U-BMMT (*Acre* sp.), which confirmed the existence of a heterogeneous interlayer[40] originated by water and uranyl cations in the interlayer.[16] Results for mathematical decomposition of d(001) reflection peak for all samples was done and resumed in Table S3 (Supporting Information).

ζ-Potential Curves in the Presence of Uranium. Figure 2B shows the ζ-potential of U-BMMT 1% (*Apha* sp.) and U-BMMT 1% (*Acre* sp.) samples. Similar curves were obtained for U-BMMT 5% samples (data not shown).

Similar ζ-potential curves were found for U-MMT and U-MMT (P5) samples until pH 7, where a slight lower or not change of the negative ζ-potential was found respect to MMT and MMT (P5) samples (Figure 2A). This behavior agreed with results obtained by XRD and confirmed the adsorption of positive uranyl ions by cation exchange in the MMT interlayer[16]

without changing the electrical status of the sample. When the pH reached the IEP value of edges, (around pH 6.5,[33]) negative sites on the surface of edges were produced, increasing the uranyl adsorption by neutralizing them, and the negative charge of the entire surface was decreased, especially in presence of P5. Particularly, at the adsorption pH studied (3.6), the uranium uptake produced a shift of the ζ-potential of around 5 to 10 mV to a lower negative ζ-potential, for MMT and *Apha* sp., respectively.

For both U-BMMTs (*Apha* sp. and *Acre* sp.) samples, uranium adsorption generated a marked decrease of negative ζ-potential values for all ranges of pH studied, with respect to those obtained for BMMTs (*Apha* sp. and *Acre* sp.) samples. The decrease of the negative surface charge with the uptake of uranium was higher in BMMT (*Apha* sp.) (of around −20 mV, at pH 3.5) than for MMT or *Apha* sp. This behavior suggests that the main adsorption sites were provided by biomass growth on the MMT external surface, in agreement with the adsorption increase respect to MMT sample (Figure 3).

Apparent Diameter of Biopolymer Particles in Presence of Uranium. Dapp values for all samples were measured from samples recovered from a high adsorption point of the isotherms (250 ppm). The increase of apparent diameter values in the presence of uranium for MMT, MMT 1% (P5), BMMT 1% (*Apha* sp.), and BMMT 1% (*Acre* sp.) samples (1800, 1600, 1800, and 3200 nm, respectively), with respect to the same samples without uranium (Table S1, Supporting Information) indicated formation of higher aggregates where electrostatic attractions were involved.

CONCLUSIONS

Complexes between MMT and fungal biomass (BMMTs) were achieved. BMMTs showed a better uranium adsorption capacity and presented better flocculation properties than both MMT and biomass alone.

Adsorption of uranium on BMMTs occurred mainly in biomass although some molecules were also placed in the BMMTs clay interlayer. The constant electric surface charge (ζ-potential) of MMT indicated low participation of the external MMT surface in uranium uptake.

The fitting of isotherms to a sigmoidal shape model indicated that uranium was incorporated to BMMTs in heterogeneous sites.

These preliminary studies conclude that these microbial biofilms−clay systems have a great potentiality for uranium biosorption processes given the high adsorption capacity and its potential ability to be adapted to a higher scale due to the nature of the materials employed.

ASSOCIATED CONTENT

Ⓢ Supporting Information

Scanning electronic microscopy of BMMT 1% (*Apha* sp.) and BMMT 5% (*Apha* sp.), calculation of values per gram of biomass from proton consumption, apparent diameter values of MMT and BMMTs without uranium, specific constants for adsorption models and mathematical decomposition of d(001) reflection peak for BMMT samples with uranium, photos representing the different coagulation capacity of systems, MMT (P5) and MMT (P5) without glucose and thiamine isotherms. This information is available free of charge via the Internet at http://pubs.acs.org.

AUTHOR INFORMATION

Corresponding Author
*Phone: +54-011-4580-7296/7289 ext. 108. E-mail: gcurut@gmail.com.

Notes

The authors declare no competing financial interest.

ACKNOWLEDGMENTS

ABBREVIATIONS

MMT, montmorillonite; *Apha* sp., *Aphanocladium* sp.; *Acre* sp., *Acremonium* sp.; BMMT 1% (*Apha* sp.), 1% montmorillonite with *Apha* sp. biopolymer; BMMT 5% (*Apha* sp.): 5% montmorillonite with *Apha* sp. biopolymer; BMMT, montmorillonite biopolymers

REFERENCES

(1) Plaza, H. C. La industria del uranio en la Argentina. *Seguridad Radiológica* **2003**, 16−21.

(2) Heikkinen, P. M.; Korkka-Niemi, K.; Lahti, M.; Salonen, V. P. Groundwater and surface water contamination in the area of the Hitura nickel mine, Western Finland. *Environ. Geol.* **2002**, *42*, 313−329.

(3) Bertolino, S. R. A.; Zimmermann, U.; Sattler, F. J. Mineralogy and geochemistry of bottom sediments from water reservoirs in the vicinity of Córdoba, Argentina: Environmental and health constraints. *Appl. Clay Sci.* **2007**, *36*, 206−220.

(4) Kalin, M.; Wheeler, W. N.; Meinrath, G. The removal of uranium from mining waste water using algal/microbial biomass. *J. Environ. Radioactiv.* **2004**, *78*, 151−177.

(5) Francis, A. J.; Gillow, J. B.; Dodge, C. J.; Harris, R.; Beveridge, T. J.; Papenguth, H. W. Uranium association with halophilic and non-halophilic bacteria and archaea. *Radiochim. Acta* **2004**, *92*, 481−488.

(6) Haas, J. R.; Bailey, E. H.; Purvis, O. W. Bioaccumulation of metals by lichens: Uptake of aqueous uranium by *Peltigera membranacea* as a function of time and pH. *Am. Mineral.* **1998**, *83*, 1494−1502.

(7) Sylwester, E. R.; Hudson, E. A.; Allen, P. G. The structure of uranium (VI) sorption complexes on silica, alumina, and montmorillonite. *Geochim. Cosmochim. Ac.* **2000**, *64*, 2431−2438.

(8) Waite, T. D.; Davis, J. A.; Payne, T. E.; Waychunas, G. A.; Xu, N. Uranium(VI) adsorption to ferrihydrite: Application of a surface complexation model. *Geochim. Cosmochim. Ac.* **1994**, *58*, 5465−5478.

(9) Volesky, B. Biosorption and me. *Water Res.* **2007**, *41*, 4017−4029.

(10) Greathouse, J. A.; Cygan, R. T. Water structure and aqueous uranyl(VI) adsorption equilibria onto external surfaces of beidellite, montmorillonite, and pyrophyllite: Results from molecular simulations. *Environ. Sci. Technol.* **2006**, *40*, 3865−3871.

(11) Abollino, O.; Aceto, M.; Malandrino, M.; Sarzanini, C.; Mentasti, E. Adsorption of heavy metals on Na-montmorillonite. Effect of pH and organic substances. *Water Res.* **2003**, *37*, 1619−1627.

(12) Bhattacharyya, K. G.; Gupta, S. S. Adsorption of a few heavy metals on natural and modified kaolinite and montmorillonite: A review. *Adv. Colloid Interface Sci.* **2008**, *140*, 114−131.

(13) Lombardi, B.; Baschini, M.; Torres Sánchez, R. M. Bentonite deposits of Northern Patagonia. *Appl. Clay Sci.* **2003**, *22*, 309−312.

(14) Wang, Y.-J.; Jia, D.-A.; Sun, R.-J.; Zhu, H.-W.; Zhou, D.-M. Adsorption and cosorption of tetracycline and copper(II) on montmorillonite as affected by solution pH. *Environ. Sci. Technol.* **2008**, *42*, 3254−3259.

(15) Greathouse, J. A.; Stellalevinsohn, H. R.; Denecke, M. A.; Bauer, A.; Pabalan, R. T. Uranyl surface complexes in a mixed-charge

montmorillonite: Monte Carlo computer simulation and polarized XAFS results. *Clays Clay Miner.* **2005**, *53*, 278−286.

(16) Tsunashima, A.; Brindley, G. W.; Bastovanov, M. Adsorption of uranium from solutions by montmorillonite: Compositions and properties of uranyl montmorillonites. *Clays Clay Miner.* **1981**, *29*, 10−16.

(17) Lagaly, G.; Bergaya, F., K., B.; G., T. Colloid clay science. In *Developments in Clay Science*; Elsevier: Oxford, 2006; Vol. *1*, Chapter 5, pp 141−245.

(18) Yang, L.; Jiang, L.; Zhou, Z.; Chen, Y.; Wang, X. The sedimentation capabilities of hexadecyltrimethylammonium-modified montmorillonites. *Chemosphere* **2002**, *48*, 461−466.

(19) Ohnuki, T.; Yoshida, T.; Ozaki, T.; Samadfam, M.; Kozai, N.; Yubuta, K.; Mitsugashira, T.; Kasama, T.; Francis, A. J. Interactions of uranium with bacteria and kaolinite clay. *Chem. Geol.* **2005**, *220*, 237−243.

(20) Iqbal, M.; Saeed, A. Biosorption of reactive dye by loofa sponge-immobilized fungal biomass of *Phanerochaete chrysosporium*. *Process Biochem.* **2007**, *42*, 1160−1164.

(21) Iborra, C. V.; Cultrone, G.; Cerezo, P.; Aguzzi, C.; Baschini, M. T.; Vallejos, J.; López-Galindo, A. Characterisation of northern *Patagonian bentonites* for pharmaceutical uses. *Appl. Clay Sci.* **2006**, *31*, 272−281.

(22) Pantanetti, M.; Dos Santos Afonso, M.; Torres Sánchez, R., M. Cambios en la adsorción del fungicida Iprodión en montmorillonita por tratamiento térmico y mecánico. In *Las Fronteras de la Física y la Química Ambiental en Ibero América*; Blesa, M.; Dos Santos Afonso, M.; M., T. S. R., Eds.; Univ. San Martín: Buenos Aires, 2008; pp 469−474.

(23) Magnoli, A. P.; Tallone, L.; Rosa, C. A. R.; Dalcero, A. M.; Chiacchiera, S. M.; Torres Sanchez, R. M. Commercial bentonites as detoxifier of broiler feed contaminated with aflatoxin. *Appl. Clay Sci.* **2008**, *40*, 63−71.

(24) Torres Sánchez, R. M.; Falasca, S. Specific surface area and surface charges of some argentinian soils. *J. Plant Nutr. Soil Sci.* **1997**, *160*, 223−226.

(25) Tournassat, C.; Ferrage, E.; Poinsignon, C.; Charlet, L. The titration of clay minerals: II. Structure-based model and implications for clay reactivity. *J. Colloid Interface Sci.* **2004**, *273*, 234−246.

(26) Yong, P.; Eccles, H.; Macaskie, L. E. Determination of uranium, thorium, and lanthanum in mixed solutions using simultaneous spectrophotometry. *Anal. Chim. Acta* **1996**, *329*, 173−179.

(27) Torres Sánchez, R. M.; Genet, M. J.; Gaigneaux, E. M.; Dos Santos Afonso, M.; Yunes, S. Benzimidazole adsorption on the external and interlayer surfaces of raw and treated montmorillonite. *Appl. Clay Sci.* **2011**, *53*, 366−373.

(28) Lagaly, G. *Tonminerale und Tone*; Steinkopff Verlag: Darmstadt, 1993.

(29) Kozaki, T.; Liu, J.; Sato, S. Diffusion mechanism of sodium ions in compacted montmorillonite under different NaCl concentration. *Phys. Chem. Earth* **2008**, *33*, 957−961.

(30) Thomas, F.; Michot, L. J.; Vantelon, D.; Montargès, E.; Prélot, B.; Cruchaudet, M.; Delon, J. F. Layer charge and electrophoretic mobility of smectites. *Colloids Surf., A* **1999**, *159*, 351−358.

(31) Holder, D. J.; Kirkland, B. H.; Lewis, M. W.; Keyhani, N. O. Surface characteristics of the entomopathogenic fungus *Beauveria (Cordyceps) bassiana*. *Microbiology* **2007**, *153*, 3448−3457.

(32) James, A. M. Charge properties of microbial cell surfaces. In *Microbial Cell Surface Analysis—Structural and Physicochemical Methods*; Mozes, N.; Handley, P. S.; Busscher, H. J.; Rouxhet, P. G., Eds.; VCH Publishers, Inc.: New York, 1991; pp 221−262.

(33) Tombacz, E.; Szekeres, M. Colloidal behavior of aqueous montmorillonite suspensions: The specific role of pH in the presence of indifferent electrolytes. *Appl. Clay Sci.* **2004**, *27*, 75−94.

(34) Solari, J. A.; Huerta, G.; Escobar, B.; Vargas, T.; Badilla-Ohlbaum, R.; Rubio, J. Interfacial phenomena affecting the adhesion of *Thiobacillus ferrooxidans* to sulphide mineral surface. *Colloids Surf.* **1992**, *69*, 159−166.

(35) Gargarello, R.; Cavalitto, S.; Di Gregorio, D.; Niello, J. F.; Huck, H.; Pardo, A.; Somacal, H.; Curutchet, G. Characterisation of uranium(VI) sorption by two environmental fungal species using gamma spectrometry. *Environ. Technol.* **2008**, *29*, 1341−1348.

(36) Wu, J.; Li, B.; Liao, J.; Feng, Y.; Zhang, D.; Zhao, J.; Wen, W.; Yang, Y.; Liu, N. Behavior and analysis of cesium adsorption on montmorillonite mineral. *J. Environ. Radioactiv.* **2009**, *100*, 914−920.

(37) Zhou, J.; Wu, P.; Dang, Z.; Zhu, N.; Li, P.; Wu, J.; Wang, X. Polymeric Fe/Zr pillared montmorillonite for the removal of Cr(VI) from aqueous solutions. *Chem. Eng. J.* **2010**, *162*, 1035−1044.

(38) Guibal, E.; Roulph, C.; Le Cloirec, P. Uranium biosorption by a filamentous fungus *Mucor miehei* pH effect on mechanisms and performances of uptake. *Water Res.* **1992**, *26*, 1139−1145.

(39) Haas, J. R.; Dichristina, T. J.; Wade, R., Jr Thermodynamics of U(VI) sorption onto *Shewanella putrefaciens*. *Chem. Geol.* **2001**, *180*, 33−54.

(40) Melkior, T.; Gaucher, E. C.; Brouard, C.; Yahiaoui, S.; Thoby, D.; Clinard, C.; Ferrage, E.; Guyonnet, D.; Tournassat, C.; Coelho, D. Na+ and HTO diffusion in compacted bentonite: Effect of surface chemistry and related texture. *J. Hydrol.* **2009**, *370*, 9−20.

2279

dx.doi.org/10.1021/ie301773p | *Ind. Eng. Chem. Res.* 2013, 52, 2273−2279